High-Dimensional Bell Test without Detection Loophole

Xiao-Min Hu,[*] Chao Zhang[®],[*] Bi-Heng Liu[®],[†] Yu Guo, Wen-Bo Xing, Cen-Xiao Huang,
Yun-Feng Huang, Chuan-Feng Li,[‡] and Guang-Can Guo

CAS Key Laboratory of Quantum Information, University of Science and Technology of China, Hefei, 230026, China;
CAS Center For Excellence in Quantum Information and Quantum Physics,
University of Science and Technology of China, Hefei, 230026, China
and Hefei National Laboratory, University of Science and Technology of China, Hefei 230088, China

Violation of Bell's inequalities shows strong conflict between quantum mechanics and local realism. Loophole-free Bell tests not only deepen understanding of quantum mechanics, but are also important foundations for device-independent (DI) tasks in quantum information. High-dimensional quantum systems offer a significant advantage over qubits for closing the detection loophole. In the symmetric scenario, a detection efficiency as low as 61.8% can be tolerated using four-dimensional states and a four-setting Bell inequality [Phys. Rev. Lett. 104, 060401 (2010)]. For the first time, we show that four-dimensional entangled photons violate a Bell inequality while closing the detection loophole in experiment. The detection efficiency of the four-dimensional entangled source is about 71.7%, and the fidelity of the state is 0.995 ± 0.001. Combining the technique of multicore fibers, the realization of loophole-free high-dimensional Bell tests and high-dimensional quantum DI technologies are promising.

Introduction.—In 1935, Einstein, Podolski, and Rosen (EPR) pointed out the inconsistency in quantum mechanics if one requires the theory to be realistic and local [1]. In quantum mechanics, nonclassical two-particle states that exhibit correlations at a spacelike distance are referred to as "entangled." Because locality and reality are so fundamental to classical intuition, there was a heated debate in the 20th century about the completeness of quantum mechanics. In 1964, Bell devised a way to, in principle, end the debate experimentally by analyzing the limit of allowed correlations between measurements done on remote particles [2]. If performed under ideal conditions, a violation of Bell's inequalities would rule out all possible local realistic theories.

Since the 1970s, violations of Bell's inequalities have been confirmed in numerical experiments, providing strong indication that nature is nonlocal [3–8]. However, imperfections in such experiments open various loopholes that could, in principle, be exploited by a local hidden variable model to predict the result [9]. There are three main loopholes in Bell tests: locality loophole (or communication loophole), freedom of choice loophole, and fair sampling loophole (or detection loophole). With the development of quantum technology, these three loopholes have been closed simultaneously in nitrogen-vacancy center systems [10], photon systems [11,12], and atom systems [13]. On one hand, loophole-free Bell tests increase understanding of the physical nature of quantum mechanics and strengthen belief in the theory. On the other hand, loophole-free Bell tests are also important foundations for

device-independent (DI) tasks in quantum information, such as DI quantum key distribution [14], DI random number generation [15], and DI state certification [16].

However, all experimental Bell tests without loopholes are focused on two-dimensional (qubit) systems, and there is no experimental research on a high-dimensional (qudit) system [17–22]. Thus far, none of the above loopholes have been closed in a high-dimensional system. Meanwhile, most physical systems in nature are in high-dimensional states with multiple quantum levels, and most high-dimensional states are entangled states [23]. Compared with qubit systems, high-dimensional quantum systems have many advantages in performing DI tasks: higher information capacity [24,25], better security in quantum communication 26]], and larger violation of Bell inequalities [27]. Like the qubit Bell tests, the high-dimensional Bell tests also have to overcome the above three loopholes. The first two loopholes can be guaranteed by keeping the spacelike separation between Alice, Bob, and the entanglement source emission. The third loophole can be closed by improving system detection efficiency to a certain bound [28,29].

It is worth noting that the efficiency requirement for closing the detection efficiency loophole in a high-dimensional system is lower than that of a qubit system. For the Clauser-Horne-Shimony-Holt (CHSH) Bell inequality (qubit case), the threshold of the detection efficiency is 82.8% for a maximally entangled qubit pair and can be lowered to 66.7% using partially entangled states in a symmetric scenario [30]. For a high-dimensional system, it has been proved that any efficiency close to $1/d$ can be
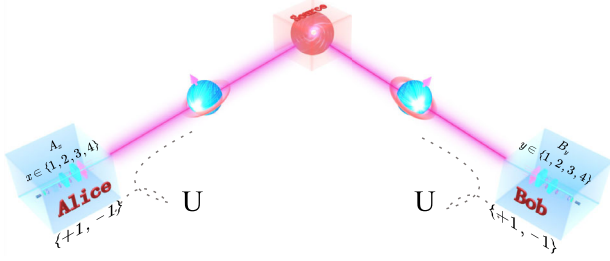
FIG. 1. Scheme of the experiment. We suppose a high-dimensional Bell-type scheme in which two distant parties, Alice and Bob, can choose measurement among four measurement settings (A_x, B_y) with binary outcomes. Alice's and Bob's outcomes are denoted by $\{+1, -1\}$. There are losses in the photon distribution and detection processes. All the lost photons are also included in the derivation of the inequality as "undetected" (U) events. The different terms of the inequality are photon counts recorded in the different settings.

tolerated using a d-dimensional system and a series of d-set Bell inequalities [31]. In the symmetric scenario, an efficiency as low as 61.8% can be tolerated using four-dimensional states and a four-setting Bell inequality [32].

Here, we report a high-dimensional path entanglement source with high detection efficiency. The fidelity of the four-dimensional maximally entangled state is 0.995 ± 0.001, and the detection efficiency of both photons is greater than 70%. For the first time, we realize the violation of four-dimensional Bell inequality without detection loophole. The new high-dimensional entangled photon source is in the communication band (1550 nm). Combined with the existing high-dimensional entanglement distribution and manipulation technologies [33–35], this raises the hope of closing all the loopholes of high-dimensional Bell tests at the same time.

Protocol.—The threshold detection efficiency can be significantly lowered using qudits [32]. As shown in Fig. 1, we consider a Bell-type scheme with two distant parties, Alice and Bob, who can choose measurement among four measurement settings with binary outcomes. Alice's settings are denoted by A_x with $x \in \{1, 2, 3, 4\}$, and her output is denoted by $a \in \{+1, -1\}$; similarly, for Bob we have B_y with $y \in \{1, 2, 3, 4\}$, and his output is denoted by $b \in \{+1, -1\}$. The experiment is characterized by the set of joint probabilities $P(A_x = a, B_y = b)$ to get outcomes a and b when A_x and B_y are measured. All these probabilities are determined by the following subset of probabilities: $P(A_x B_y) = p(A_x = 1, B_y = 1)$, $P(A_x) = P(A_x = 1)$, and $P(B_y) = P(B_y = 1)$, which are thus sufficient to consider.

We consider the Bell inequality $I_{4422}^4 < 0$ introduced in Ref. [36], which can be rewritten as

$$I_{4422}^4 = I_{\text{CH}}^{(1,2;1,2)} + I_{\text{CH}}^{(3,4;3,4)} - I_{\text{CH}}^{(2,1;4,3)} - I_{\text{CH}}^{(4,3;2,1)}$$
$$- P(A_2) - P(A_4) - P(B_2) - P(B_4), \quad (1)$$

where $I_{\text{CH}}^{(i,j;m,n)} \equiv P(A_i, B_m) + P(A_j, B_m) + P(A_i, B_n) - P(A_j, B_n) - P(A_i) - P(B_m)$. In experiment, one records measurements of single counts (S) (number of detection events on one side) and coincidence counts (C) (number of detected pairs). Let $C(A_x, B_y)$ denote the coincidence counts for Alice and Bob when they measured in setting A_x, B_y, and $S(A_x)$ [$S(B_y)$] denotes the single counts for Alice (Bob) when she (he) measured in setting A_x (B_y). Then, we can rewrite the inequality $J_{4422}^4 < 0$ as

$$J_{4422}^4 = N \times I_{\text{CH}}^{(1,2;1,2)} + N \times I_{\text{CH}}^{(3,4;3,4)} - N \times I_{\text{CH}}^{(2,1;4,3)}$$
$$- N \times I_{\text{CH}}^{(4,3;2,1)} - S(A_2) - S(A_4) - S(B_2) - S(B_4), \quad (2)$$

where $N \times I_{\text{CH}}^{(i,j;m,n)} \equiv C(A_i, B_m) + C(A_j, B_m) + C(A_i, B_n) - C(A_j, B_n) - S(A_i) - S(B_m)$, and N denotes the total number of entanglement pairs. Remarkably, Alice and Bob each need only one detector to test the Clauser-Horne (CH) inequality. We consider the symmetric case, in which the detection efficiency of Alice and Bob is $\eta_A = \eta_B = \eta$. The correlation term in the inequality should be corrected according to $C(A_i, B_j) \to \eta^2 C(A_i, B_j)$, $S(A_i) \to \eta S(A_i)$, and $S(B_i) \to \eta S(B_i)$. Inserting these terms into Eq. (2), we obtain the detection-efficiency-dependent Bell inequality $J_{4422}(\eta) < 0$.

Similar to the two-dimensional Bell test without detection loophole, the maximally entangled state is not the best choice to close the detection loophole. The four-dimensional entangled state is written in the Schmidt form as [32]

$$|\psi_\epsilon^4\rangle = \sqrt{\frac{1 - \epsilon^2}{3}}(|0\rangle|0\rangle + |1\rangle|1\rangle + |2\rangle|2\rangle) + \epsilon|3\rangle|3\rangle, \quad (3)$$

with $\epsilon \in [0, 1]$. In the limit $\epsilon \to 0$, the inequality $J_{4422}^4(\eta) \leq 0$ is violated if $\eta > (\sqrt{5} - 1)/2 \simeq 0.618$. For the maximally entangled state ($\epsilon = \frac{1}{2}$), an efficiency of 77.0% can be tolerated. These results represent a significant improvement over the best values for qubit systems [30].

Experimental scheme.—The experimental setup is shown in Fig. 2. First, a continuous-wave (cw) laser with a wavelength of 775 nm and a power of 300 mW is separated to four paths to pump a 6.3-mm-thick beamlike cut β-barium-borate (BBO) crystal to generate a two-photon four-dimensional state $|\Phi_4\rangle = C_1|00\rangle + C_2|11\rangle + C_3|22\rangle + C_4|33\rangle$ (no normalization) [37]. Then, this two-photon state is distributed to Alice and Bob and measured locally. Beam displacers (BDs) operating at 775 nm introduce a 4 mm separation between the horizontally and vertically polarized photons.

Generally, owing to momentum conservation in spontaneous parametric down-conversion, a decrease in momentum uncertainty of the pump beam can lead to a higher
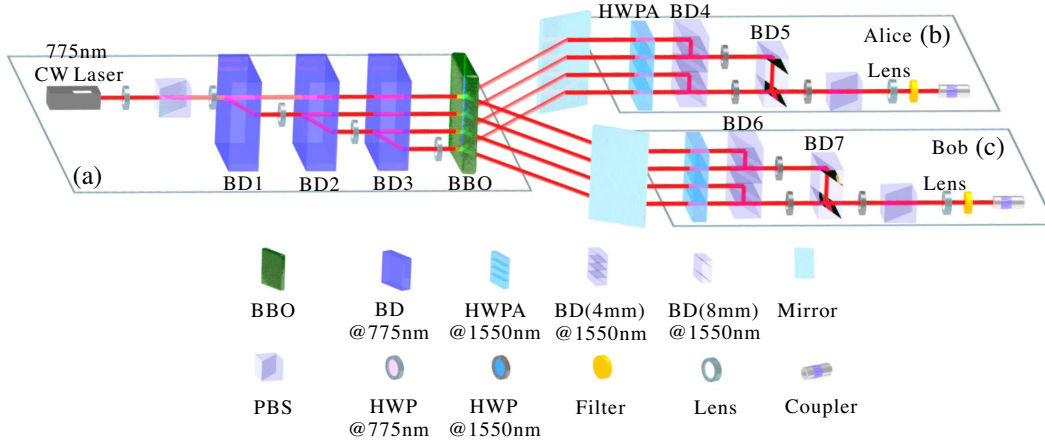
FIG. 2. Experimental setup. (a) Four-dimensional entanglement source with high detection efficiency. The pump light is a 775 nm cw light with a power of 300 mW. Four parallel pump beams are generated by operating a half wave plate (HWP) and beam displacers (BD1–BD3). By adjusting the angles of the HWPs, the energy of the pump beam can be divided into any proportion. Then, four beams of light effect spontaneous parametric down-conversion of the beamlike cut BBO crystal ($|H\rangle_{775\,nm} \to |H\rangle_{1550\,nm} \otimes |V\rangle_{1550\,nm}$). We encode each path from top to bottom as ($|0\rangle, |1\rangle, |2\rangle, |3\rangle$) and can thus obtain the four-dimensional entangled state $|\Phi_4\rangle = C_1|00\rangle + C_2|11\rangle + C_3|22\rangle + C_4|33\rangle$ ($C_1^2 + C_2^2 + C_3^2 + C_4^2 = 1$). (b),(c) Measurement setup. The measurement setup consists of a half wave plate array (HWPA), HWPs, BDs, and a polarizing beam splitter (PBS). The HWPA consists of 0° and 45° HWPs intervals and is used to modulate the polarization state of the four paths. Through the polarization control of the HWPs and BD4-BD5, different projection measurements can be performed as described in detail in the Supplemental Material [38]. BD4 and BD5 can shift the beam by 4 and 8 mm, respectively. To reduce the loss of 1550 nm light, the material used in measurement setup is H-ZF13 glass with low absorption at 1550 nm. The waist spot diameter of the pump light and the collection system on the crystal are 1.20 and 0.56 mm, respectively, to ensure effective matching between the pump system and the collection system.

collection efficiency [39]. Therefore, a larger pump beam waist could result in a high collection efficiency. However, an excessively large pump beam waist will rapidly reduce the brightness of photon pairs. Thus, there is a trade-off between the collection efficiency and the photon brightness. Consequently, the pump beam waist was chosen as 1.20 mm in our experiment. In the above case, we estimated the effect of walk-off of down-converted 1550 nm photons in the BBO crystal. This walk-off comes from the constant parametric down-conversion of the pump light during crystal propagation, which cannot be effectively compensated. The walking distance is about 400 μm in a 6.3-mm-thick BBO crystal. We calculated the overlap between the walk-off wave packet and the standard Gaussian wave packet, which exceeded 0.95; thus we can conclude that the walk-off has a limited impact on the detection efficiency. To match with the pump system, we selected a collecting lens with a focal length of 40 cm, and the waist spot diameter on the crystal was 0.56 mm. A bandpass filter (1550 ± 15 nm) and a long-pass filter (1200 nm) were used to remove the small sidebands. The transmittance of the two filters were both more than 0.99. The working temperature of the superconducting detector was 2.2 K, and the photon detection efficiency was 90%. We obtained a two-photon count rate of 350 Hz/mW and a detection efficiency of 75.2 ± 0.1% in the case of direct coupling.

The measurement setup for high-dimensional entangled states needs more optical elements than the two-dimensional detection loophole-free experiment [28,29], so we need to optimize each optical element. In addition to coating each optical element with a broadband 1550 nm high-transmittance film, we selected H-ZF13 glass with very low absorption at 1550 nm as the substrate of the optical elements. We arrive at a final detection efficiency of 71.8 ± 0.1% in Alice's arm and 71.6 ± 0.1% in Bob's arm, sufficient to violate a Bell inequality without detection loophole. These efficiencies represent a ratio of coincidence events divided by single counts (i.e., total events measured in one detector) measured directly over the entire system and not corrected for any losses. We attribute these imperfect detection efficiencies to various possible effects, including optical losses in the source, coupling, fiber splices, optical elements, and detectors. The HWP before each BD can control the amplitude of each path. We can adjust the angles of these HWPs to prepare the entangled states required by the experiment. Meanwhile, the phase difference between each path subspace can be realized by tilting BDs and HWPs. Taking $|0\rangle$ and $|1\rangle$ subspaces as an example, the phase difference can be confirmed by measuring the $(|0\rangle + |1\rangle)/\sqrt{2}$ and $(|0\rangle - |1\rangle)/\sqrt{2}$ bases. Thus, we can prepare the required entangled states accurately. The four-dimensional maximally entangled quantum state and four-dimensional state (3) with $\epsilon = 0.219$ generated by our scheme can be characterized via the quantum state fidelity witness [20]. The fidelities of these four-dimensional entangled states both are 0.995 ± 0.001.
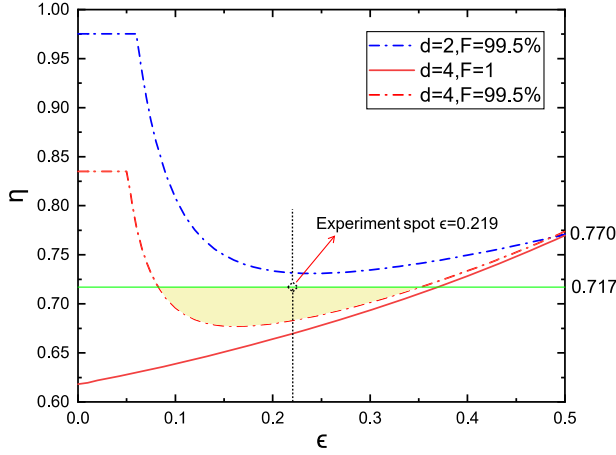
FIG. 3. Detection efficiency threshold for the symmetric Bell test without detection loophole. Threshold efficiency η as a function of the degree of entanglement ϵ for $F = 0.995$. The four-dimensional quantum state ($d = 4$) is defined in the Schmidt form as Eq. (3) (red dotted line) for the I^4_{4422} inequality [32], and the qubit quantum state ($d = 2$) is defined in the Schmidt form as $|\psi^2_\epsilon\rangle = \sqrt{1 - \epsilon^2}|0\rangle|0\rangle + \epsilon|1\rangle|1\rangle$ (blue dotted line) for the CHSH inequality [30]. The yellow area is the area that can be effectively violated in our case. After numerical optimization, the violation of I^4_{4422} is greatest when $\epsilon = 0.219$. The red solid line represents very partially entered states ($\epsilon \to 0$). The efficiency drops to 61.8% when the fidelity is $F = 1$ in the four-dimensional case.

For the two-dimensional subspace, the visibility of the computational basis ($\{|0\rangle, |1\rangle\}$) is 0.999 ± 0.001, and the visibility of the Fourier basis [$\{1/\sqrt{2}(|0\rangle + |1\rangle)$, $1/\sqrt{2}(|0\rangle - |1\rangle)\}$] is 0.995 ± 0.001.

The optimal value for ϵ can be obtained according to the fidelity of entangled states and the photon detection efficiency. As shown in Fig. 3, the existing experimental setup can get effective violation in the region $\epsilon \in [0.083, 0.351]$. To simplify the experimental setup, we define Alice's and Bob's measurement settings with the following four-dimensional unit vectors [32]:

$$A_1 = (-u, -u, \vec{p}_1), \qquad A_3 = (u, u, \vec{p}_1),$$
$$A_2 = (-v, v, \vec{p}_2), \qquad A_4 = (v, -v, \vec{p}_2),$$
$$B_1 = (-u, u, \vec{q}_1), \qquad B_3 = (u, -u, \vec{q}_1),$$
$$B_2 = (-v, -v, \vec{q}_2), \qquad B_4 = (v, v, \vec{q}_2), \qquad (4)$$

where $\vec{p}$, $\vec{q}$ are two-dimensional vectors, and $\vec{p}_i = (p_{i1}, p_{i2}), \vec{q}_i = (q_{i1}, q_{i2})$ for $i = 1, 2$. The most statistically significant violation of local reality for our system can be optimized according to the state fidelity and detection efficiency (see the Supplemental Material [38]). We set the state with a value of 0.219 for ϵ. Alice and Bob selected the following measurement basis:

$$A_1 = \begin{pmatrix} 0.161 \\ 0.161 \\ 0.044 \\ 0.973 \end{pmatrix}, \qquad A_2 = \begin{pmatrix} -0.510 \\ 0.510 \\ 0.308 \\ -0.621 \end{pmatrix}, \qquad (5)$$

$$A_3 = \begin{pmatrix} 0.161 \\ 0.161 \\ -0.044 \\ -0.973 \end{pmatrix}, \qquad A_4 = \begin{pmatrix} 0.510 \\ -0.510 \\ 0.308 \\ -0.621 \end{pmatrix}, \qquad (6)$$

$$B_1 = \begin{pmatrix} -0.161 \\ 0.161 \\ 0.044 \\ -0.973 \end{pmatrix}, \qquad B_2 = \begin{pmatrix} 0.510 \\ 0.510 \\ 0.308 \\ 0.621 \end{pmatrix}, \qquad (7)$$

$$B_3 = \begin{pmatrix} 0.161 \\ -0.161 \\ 0.044 \\ -0.973 \end{pmatrix}, \qquad B_4 = \begin{pmatrix} 0.510 \\ 0.510 \\ -0.308 \\ -0.621 \end{pmatrix}. \qquad (8)$$

Experimental result.—After recording for a total of 500 s per setting (Table I), we divided our data into 10 s blocks and calculated the standard deviation of the resulting 50 different J^4_{4422} values. To reduce the statistical error of data, we average the measured four single counts of $A_i(B_i)$ as the calculation data in I^4_{4422}. Thus, we selected $\overline{S(A_i)} = \sum_{j=1}^4 S(A_i|A_iB_j)/4$ and $\overline{S(B_j)} = \sum_{i=1}^4 S(B_j|A_iB_j)/4$ [29]. This yielded $\sigma = 602$ for the average J^4_{4422} value of $J^4_{4422}(\text{average}) = 8688$, a 14σ violation. The total coincidence number of the 10 s photon source is $C = 946\,790$,

TABLE I. Measurement results. A total measurement time is 500 s per setting.

Settings	Singles (A)	Coincidences	Singles (B)
A_1B_1	4 203 655	2 014 238	4 297 946
A_1B_2	4 181 758	2 553 313	14 038 231
A_1B_3	4 245 350	2 067 573	4 282 990
A_1B_4	4 206 615	133 104	14 286 595
A_2B_1	13 907 983	2 491 274	4 298 855
A_2B_2	14 199 547	69 098	14 057 509
A_2B_3	13 883 568	111 561	4 318 151
A_2B_4	14 118 259	82 190	14 318 967
A_3B_1	4 232 556	2 069 013	4 312 923
A_3B_2	4 246 346	125 051	14 111 767
A_3B_3	4 223 718	2 018 391	4 282 947
A_3B_4	4 231 994	2 530 176	13 936 418
A_4B_1	14 251 918	109 579	4 289 505
A_4B_2	13 948 666	71 746	13 998 204
A_4B_3	13 943 370	2 490 319	4 290 286
A_4B_4	13 937 483	61 194	14 488 876

when the photon detection efficiencies of Alice and Bob are combined. We estimate the number of produced pairs as $N = 1\,842\,716$ per applied setting. Thus, we can calculate the violation of the normalized inequality to be $I^4_{4422}(\text{average}) = 0.004\,72 \pm 0.000\,33$. Our results agree well with those predicted using our entangled state and photon detection efficiency after we account for the measured background and fluorescence noise.

As shown in Fig. 3, the four-dimensional entangled state has a higher detection efficiency tolerance than the two-dimensional entangled state under the same fidelity. It is worth noting that, in the case of our experimental fidelity and detection efficiency, the violations cannot be achieved in the two-dimensional case [30], but can be effectively violated in the four-dimensional case [30].

Discussion.—We have presented new high-dimensional entangled photon pair generation, collection, and measurement technologies with high detection efficiency. We have experimentally implemented a four-dimensional entangled source with a detection efficiency of about 71.7% and, for the first time, successfully violated a high-dimensional Bell inequality (I^4_{4422}) without detection loophole.

Eliminating all loopholes from the Bell inequality test requires not only closing the detection loophole, but also introducing spacelike separation to avoid potential communication between Alice, Bob, and the entangled source emission event. The two-dimensional Bell inequality without loopholes has been realized in solid-state, atomic, and photonic systems. Compared with two-dimensional systems, high-dimensional quantum systems have many advantages, but the structure is more complex. First, we need to achieve long-distance and high-quality high-dimensional entangled state distribution. Second, we need a high-speed random number generator, high-speed high-dimensional measurement system, and precise timing. Therefore, implementing a high-dimensional loophole-free Bell test requires high-dimensional entanglement distribution and high-speed operations. The degrees of freedom (DOF) needed to achieve high-dimensional entanglement in photonic systems are orbital angular momentum (OAM) [17], time bin [18] and path DOF [19,20,35]. However, for the DOF of OAM and time bin, the drawback is low state fidelity and postselected measurement, respectively. Therefore, the most promising way to close the three loopholes simultaneously is the path DOF with existing technology [38]. It is worth noting that the high-dimensional path entanglement source we developed is in the communication band (1550 nm) and can be distributed through optical fibers with low loss. Of course, both the entanglement distribution and high-speed high-dimensional operation will introduce photon loss, so the detection efficiency of the system needs to be further optimized. EPR steering only needs to ensure that the detection loophole is closed on one side, so the threshold detection efficiency is significantly lower than that of a Bell test [40]. Therefore, high-dimensional loophole-free EPR steering will probably be realized first. With the development of high-dimensional system operation in recent years, the prospect of implementing a high-dimensional loophole-free experiment seems very promising.

---

[*]X.-M. H. and C. Z. contributed equally to this work.
[†]bhliu@ustc.edu.cn
[‡]cfli@ustc.edu.cn

[1] A. Einstein, B. Podolsky, and N. Rosen, Phys. Rev. 47, 777 (1935).
[2] J. S. Bell, Phys. Phys. Fiz. 1, 195 (1964).
[3] S. J. Freedman and J. F. Clauser, Phys. Rev. Lett. 28, 938 (1972).
[4] A. Aspect, J. Dalibard, and G. Roger, Phys. Rev. Lett. 49, 1804 (1982).
[5] Z. Y. Ou and L. Mandel, Phys. Rev. Lett. 61, 50 (1988).
[6] G. Weihs, T. Jennewein, C. Simon, H. Weinfurter, and A. Zeilinger, Phys. Rev. Lett. 81, 5039 (1998).
[7] M. A. Rowe, D. Kielpinski, V. Meyer, C. A. Sackett, W. M. Itano, C. Monroe, and D. J. Wineland, Nature (London) 409, 791 (2001).
[8] J. Hofmann, M. Krug, N. Ortegel, L. Gérard, M. Weber, W. Rosenfeld, and H. Weinfurter, Science 337, 72 (2012).
[9] J.-Å. Larsson, J. Phys. A 47, 424003 (2014).
[10] B. Hensen, H. Bernien, A. E. Dréau, A. Reiserer, N. Kalb, M. S. Blok, J. Ruitenberg, R. F. Vermeulen, R. N. Schouten, C. Abellán et al., Nature (London) 526, 682 (2015).
[11] M. Giustina et al., Phys. Rev. Lett. 115, 250401 (2015).
[12] L. K. Shalm et al., Phys. Rev. Lett. 115, 250402 (2015).
[13] W. Rosenfeld, D. Burchardt, R. Garthoff, K. Redeker, N. Ortegel, M. Rau, and H. Weinfurter, Phys. Rev. Lett. 119, 010402 (2017).
[14] A. Acín, N. Brunner, N. Gisin, S. Massar, S. Pironio, and V. Scarani, Phys. Rev. Lett. 98, 230501 (2007).
[15] Y. Liu, Q. Zhao, M.-H. Li, J.-Y. Guan, Y. Zhang, B. Bai, W. Zhang, W.-Z. Liu, C. Wu, X. Yuan et al., Nature (London) 562, 548 (2018).
[16] T. H. Yang, T. Vértesi, J.-D. Bancal, V. Scarani, and M. Navascués, Phys. Rev. Lett. 113, 040401 (2014).
[17] A. Mair, A. Vaziri, G. Weihs, and A. Zeilinger, Nature (London) 412, 313 (2001).

[18] A. Martin, T. Guerreiro, A. Tiranov, S. Designolle, F. Fröwis, N. Brunner, M. Huber, and N. Gisin, Phys. Rev. Lett. **118**, 110501 (2017).

[19] J. Wang, S. Paesani, Y. Ding, R. Santagati, P. Skrzypczyk, A. Salavrakos, J. Tura, R. Augusiak, L. Mančinska, D. Bacco *et al.*, Science **360**, 285 (2018).

[20] X.-M. Hu, W.-B. Xing, B.-H. Liu, Y.-F. Huang, C.-F. Li, G.-C. Guo, P. Erker, and M. Huber, Phys. Rev. Lett. **125**, 090503 (2020).

[21] H. Xu, C. Song, W. Liu, G. Xue, F. Su, H. Deng, Y. Tian, D. Zheng, S. Han, Y.-P. Zhong *et al.*, Nat. Commun. **7**, 1 (2016).

[22] F. M. Leupold, M. Malinowski, C. Zhang, V. Negnevitsky, J. Alonso, J. P. Home, and A. Cabello, Phys. Rev. Lett. **120**, 180401 (2018).

[23] M. Weilenmann, B. Dive, D. Trillo, E. A. Aguilar, and M. Navascués, Phys. Rev. Lett. **124**, 200502 (2020).

[24] A. Tavakoli, M. Farkas, D. Rosset, J.-D. Bancal, and J. Kaniewski, Sci. Adv. **7**, eabc3847 (2021).

[25] Y. Guo, S. Cheng, X. Hu, B.-H. Liu, E.-M. Huang, Y.-F. Huang, C.-F. Li, G.-C. Guo, and E. G. Cavalcanti, Phys. Rev. Lett. **123**, 170402 (2019).

[26] L. Sheridan and V. Scarani, Phys. Rev. A **82**, 030301(R) (2010).

[27] D. Collins, N. Gisin, N. Linden, S. Massar, and S. Popescu, Phys. Rev. Lett. **88**, 040404 (2002).

[28] M. Giustina, A. Mech, S. Ramelow, B. Wittmann, J. Kofler, J. Beyer, A. Lita, B. Calkins, T. Gerrits, S. W. Nam *et al.*, Nature (London) **497**, 227 (2013).

[29] B. G. Christensen, K. T. McCusker, J. B. Altepeter, B. Calkins, T. Gerrits, A. E. Lita, A. Miller, L. K. Shalm, Y. Zhang, S. W. Nam, N. Brunner, C. C. W. Lim, N. Gisin, and P. G. Kwiat, Phys. Rev. Lett. **111**, 130406 (2013).

[30] P. H. Eberhard, Phys. Rev. A **47**, R747 (1993).

[31] S. Massar and S. Pironio, Phys. Rev. A **68**, 062109 (2003).

[32] T. Vértesi, S. Pironio, and N. Brunner, Phys. Rev. Lett. **104**, 060401 (2010).

[33] X.-M. Hu, W.-B. Xing, B.-H. Liu, D.-Y. He, H. Cao, Y. Guo, C. Zhang, H. Zhang, Y.-F. Huang, C.-F. Li, and G.-C. Guo, Optica **7**, 738 (2020).

[34] Y. Ding, D. Bacco, K. Dalgaard, X. Cai, X. Zhou, K. Rottwitt, and L. K. Oxenløwe, npj Quantum Inf. **3**, 25 (2017).

[35] E. S. Gómez, S. Gómez, I. Machuca, A. Cabello, S. Pádua, S. P. Walborn, and G. Lima, Phys. Rev. Applied **15**, 034024 (2021).

[36] N. Brunner and N. Gisin, Phys. Lett. A **372**, 3162 (2008).

[37] X.-M. Hu, J.-S. Chen, B.-H. Liu, Y. Guo, Y.-F. Huang, Z.-Q. Zhou, Y.-J. Han, C.-F. Li, and G.-C. Guo, Phys. Rev. Lett. **117**, 170403 (2016).

[38] See Supplemental Material at http://link.aps.org/supplemental/10.1103/PhysRevLett.129.060402 for more experimental details and discussions.

[39] P. B. Dixon, D. Rosenberg, V. Stelmakh, M. E. Grein, R. S. Bennink, E. A. Dauler, A. J. Kerman, R. J. Molnar, and F. N. C. Wong, Phys. Rev. A **90**, 043804 (2014).

[40] B. Wittmann, S. Ramelow, F. Steinlechner, N. K. Langford, N. Brunner, H. M. Wiseman, R. Ursin, and A. Zeilinger, New J. Phys. **14**, 053030 (2012).